Entrance channel effects in fission of ^{197}Tl

Hardev Singh,* Ajay Kumar, Bivash R. Behera, and I. M. Govil
Department of Physics, Panjab University, Chandigarh 160014, India

K. S. Golda, Pankaj Kumar, Akhil Jhingan, R. P. Singh, P. Sugathan, M. B. Chatterjee, and S. K. Datta
Inter University Accelerator Centre, New Delhi 110067, India

Ranjeet
Department of Physics and Astrophysics, Delhi University, Delhi 110007, India

Santanu Pal
Variable Energy Cyclotron Centre, 1/AF, Bidhan Nagar, Kolkata 700064, India

G. Viesti
Dipartimento di Fisica and Sezione INFN Padova, I-35131 Padova, Italy
(Received 24 March 2007; revised manuscript received 25 June 2007; published 26 October 2007)

The pre- and post-scission neutron multiplicities are measured for ^{16}O + ^{181}Ta and ^{19}F + ^{178}Hf systems where the same compound nucleus ^{197}Tl is formed at the same excitation energies ($E^* = 72$, 76, and 81 MeV). The measured pre-scission neutron multiplicities are found to be different for the two reactions and this difference in neutron yield increases with the excitation energy of the compound nucleus. The experimental pre-scission neutron yield is compared with predictions from the statistical model of compound nuclear decay containing the strength of nuclear viscosity as a free parameter. The magnitude of nuclear viscosity required to fit the experimental yield is found to be different for the two reactions. Because the two systems under consideration lie on the two sides of the Businaro-Gallone point, this observation indicates that the entrance channel mass asymmetry plays an important role in determining the number of neutrons emitted prior to scission in fusion-fission reactions.

DOI: 10.1103/PhysRevC.76.044610 PACS number(s): 25.70.Jj, 25.70.Gh, 24.10.Pa, 27.80.+w

I. INTRODUCTION

The fission of an atomic nucleus is a unique process in which a nuclear collective motion sets in involving all the nucleons in the nucleus and where a large number of nucleons are eventually transported across the fission barrier. A single nucleus splits into two during fission while undergoing a drastic change of shape from the equilibrium configuration to that in scission. Fission cross sections of highly excited compound nuclei and pre-scission multiplicities of neutrons [1–9], light charged particles [10–14], and GDR γ rays [15–20] have been measured in the past to investigate the dynamics of fission. It is now established from all these studies that the measured values of pre-scission multiplicities of light particles and γ rays are substantially higher than the standard statistical model predictions.

The enhancement in the number of the pre-scission neutrons (and other light particles and γ rays) immediately points to a slowing down of the fission process compared to the statistical model fission rate as given by Bohr and Wheeler [21]. Dynamical models are now considered essential to describe fission of highly excited nuclei usually formed in heavy ion collisions. In a dynamical model, the fission process is viewed as that of a Brownian particle in a viscous fluid. The degree of enhancement of pre-scission neutron multiplicity therefore depends on the strength of nuclear viscosity or the dissipative property of the nuclear bulk.

The pre-scission neutrons can be emitted at different stages of the fusion-fission process. If fission is considered as a quasistationary diffusion process over the fission barrier, a transient time is required for the system to build up a quasistationary probability flow over the barrier. During this transition time, the fission process is inhibited though neutrons can be emitted. Thus the neutrons emitted during the transient time partially account for the enhancement of pre-scission multiplicity of neutrons. After a quasistationary flow across the barrier is established, the fission rate is obtained from the works of Kramers [22]. The Kramers fission width depends on nuclear dissipation and is smaller than the Bohr-Wheeler fission width [21]. Thus more neutrons can be emitted in the dynamical model of fission than are predicted by the statistical model. This description however applies until the compound nucleus (CN) crosses the saddle point. Beyond the saddle point, neutron evaporation from the CN can still continue till it reaches the scission point. These saddle-to-scission neutrons make an additional contribution to the pre-scission neutron enhancement.

These different stages of neutron emission however become effective only after a fully equilibrated CN is formed. In heavy-ion-induced fusion reactions, the dinuclear system that is formed in the entrance channel subsequently evolves toward

*hardev_pu@hotmail.com

the compound nuclear system. The time scale of energy equilibration in the dinuclear system is known to be much faster than the time scale of full equilibration [3]. It is therefore possible that the energy equilibrated dinuclear system can emit neutrons before the fully equilibrated CN is formed. Thus the neutrons emitted during the CN formation time also contribute to the number of pre-scission neutrons. It is evident that the multiplicity of the formation-time neutrons depends on the entrance channel dynamics of the projectile-target system. It is known [23–25] that the dynamical evolution of an energy-equilibrated dinuclear system toward the CN for a given projectile-target system depends on the entrance channel mass asymmetry $\alpha = (A_t - A_p)/(A_t + A_p)$. It is further known that the fusion paths followed by two composite systems with $\alpha < \alpha_{BG}$ and $\alpha > \alpha_{BG}$, where α_{BG} is the critical Businaro-Gallone mass asymmetry [26], are quite different even though both systems are chosen to form the same CN.

Though a substantial amount of work has been done in the past on the measurement of multiplicity of pre-scission neutrons, the number of experimental investigations focusing on the role of entrance channel mass asymmetry in pre-scission neutron multiplicity is rather limited. Saxena *et al.* [3] studied the pre-scission neutron multiplicity by populating ^{248}Cf through two different entrance channels lying on either side of the critical Businaro-Gallone mass asymmetry and found more pre-scission neutrons from the system $^{16}O + ^{232}Th$ ($\alpha < \alpha_{BG}$) than from $^{11}B + ^{237}Np$ ($\alpha > \alpha_{BG}$).

In the present work, we have measured the pre-scission neutron multiplicity from $^{16}O + ^{181}Ta$ ($\alpha = 0.837$) and $^{19}F + ^{178}Hf$ ($\alpha = 0.807$) reactions lying on the two sides of the Businaro-Gallone point ($\alpha_{BG} = 0.814$). The measurements are made at different laboratory energies, which are chosen such that the ^{197}Tl compound nucleus is formed at the same excitation energies in the two reactions. We shall make a detailed comparison of the measured values with statistical model predictions. Our aim here is to extract evidence for entrance channel dependence of pre-scission neutron multiplicity for the systems under consideration.

II. EXPERIMENTAL DETAILS

The experiment was performed at the 15UD Pelletron of the Inter University Accelerator Centre, New Delhi. Pulsed beams of ^{16}O ($E_{lab} = 105$, 110, and 115 MeV) and ^{19}F ($E_{lab} = 108$, 113, and 118 MeV) at 4-MHz repetition rate with 1-ns width were used in the experiment. A high vacuum evaporation technique was used to prepare targets of ^{181}Ta and ^{178}Hf having thicknesses of 320 and 270 μg/cm^2, respectively. A carbon backing of 20 μg/cm^2 thickness was used for both targets. The targets were mounted at the center of a 1.5-m-diameter general purpose scattering chamber (GPSC) and were placed at -45° with respect to the beam direction. A schematic diagram of the experimental setup is shown in Fig. 1. The fission fragments were detected by using two large-area (20 × 10 cm) position-sensitive multiwire proportional counters (MWPCs) [27]. These detectors measure the position, time of flight, and energy loss of fission fragments. They were placed on movable arms on both sides of the beam at distances of 60 and 50 cm, respectively, from the target and at mean angles of 90° and -62° with respect to the beam direction to cover the folding angle for symmetric fission. The positions of these detectors were adjusted according to the folding angle depending upon the beam energies and projectile-target combination.

The neutrons were detected in coincidence with fission events by four neutron detectors, which consisted of (12.7 cm diam. ×12.7 cm thick) organic liquid scintillator cells (BC501) coupled to 12.7-cm XP4512B photomultiplier tubes, and were placed outside the scattering chamber at a distance of 100 cm from the target. Thin flanges of 3-mm-thick stainless steel (SS) were used with the scattering chamber to minimize neutron scattering. These detectors were placed at angles of 30°, 60°, 90°, and 120° with respect to the beam direction. The neutron detector array threshold was kept at about 120 keVee by calibrating it with standard γ sources (^{137}Cs and ^{60}Co) [28]. The beam flux was normalized by detecting the elastically scattered beam particles at $\pm 11^\circ$ by two silicon surface barrier detectors. The data collection was triggered when a fission fragment was detected in any one of the MWPCs and the

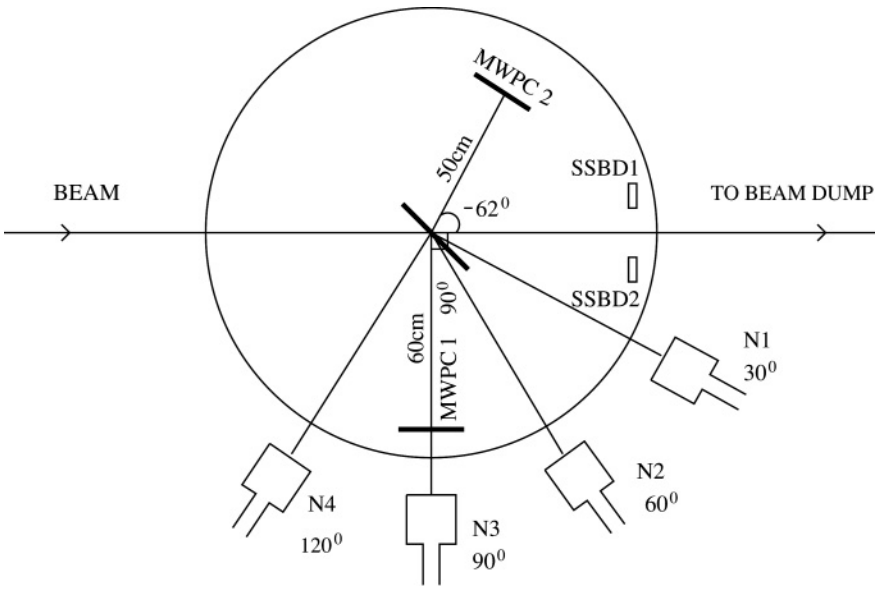

FIG. 1. Schematic of experimental setup.

time of flight (TOF) of fission fragments and neutrons were recorded in event mode for off-line analysis. The positions (X_1, Y_1, X_2, Y_2) and energy loss $(\Delta E1, \Delta E2)$ of the fission fragments were also recorded. A TOF spectrum was also generated between the elastically scattered incident particles and the radio frequency signal to monitor the timing structure of the pulsed beam. Discrimination between neutrons and γ rays was made by using pulse shape discrimination (PSD) based on the zero-crossing technique and the TOF. Because of the requirement of minimum background in the neutron spectra, the beam was dumped 3 m downstream from the target and the beam dump was well shielded with lead and borated paraffin. Data were also taken with a blank target to estimate the level of background in the neutron spectra and it was found to be negligible. The TOF of neutrons was converted into neutron energy by considering the prompt γ peak in the TOF spectrum for time calibration. The efficiency curve of the neutron detector as a function of neutron energy was obtained by using the Monte Carlo computer code MODEFF [29]. The Monte Carlo calculations, in turn, were verified by measuring the relative efficiency of the detector by using a ^{252}Cf spontaneous fission source [30].

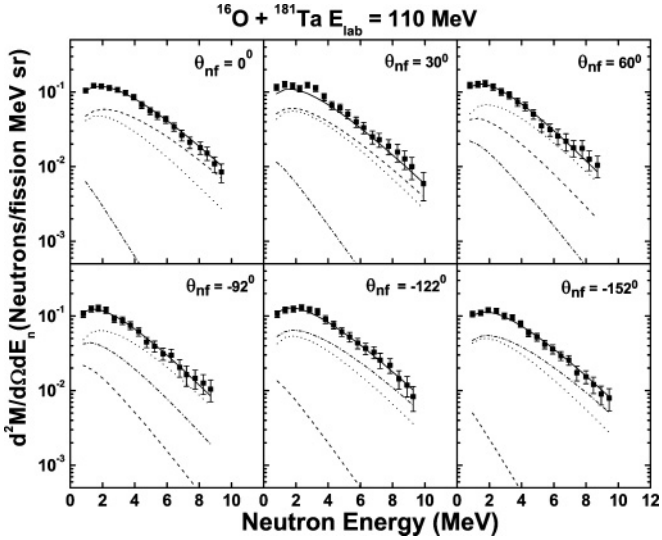

FIG. 2. Neutron multiplicity spectra (filled squares) for the ^{16}O + ^{181}Ta reaction at $E_{lab} = 110$ MeV along with the fits for the pre-scission (dotted curve) and post-scission from one fragment (dashed curve) and that from the other (dot dashed curve). The solid curve represents the total contribution.

III. DATA ANALYSIS

The pre- and post-scission components of neutron multiplicities were obtained from the measured neutron energy spectra by using a multiple source least-square fitting procedure [1]. Three moving sources of neutrons (The CN plus two fully accelerated fission fragments) were considered while calculating the multiplicities. The neutrons emitted from these moving sources were assumed to be isotropic in their respective rest frames. Thus the measured neutron multiplicities are given as

$$\frac{d^2M_n}{dE_n d\Omega_n} = \frac{M_n^{\mathrm{pre}} E_n}{4\pi (T^{\mathrm{pre}})^2} \times \exp\left[-\frac{E_n - 2\sqrt{E_n E_C/A_C}\cos\theta_C + E_C/A_C}{T^{\mathrm{pre}}}\right] + \sum_{i=1}^{2} \frac{M_{n,i}^{\mathrm{post}}\sqrt{E_n}}{2(\pi T^{\mathrm{post}})^{3/2}} \times \exp\left[-\frac{E_n - 2\sqrt{E_n E_i/A_i}\cos\theta_i + E_i/A_i}{T^{\mathrm{post}}}\right]. \quad (1)$$

where A_C and E_C are the mass and recoil energy, respectively, of the CN, A_i and E_i are the masses and kinetic energies, respectively, of the respective fission fragments, θ_C and θ_i represent the neutron detection angles measured, respectively, from the directions of the CN and the two fission fragments, and E_n is the neutron energy in the laboratory frame and T^{pre} and T^{post} are the pre- and post-scission nuclear temperatures. The calculations for the kinetic energies of the fission fragments and the folding angles were performed using the Viola [31] systematics for symmetric fission. The angular acceptance of both the neutron detectors and the fission detectors were taken into account while calculating the relative angle between the neutron and the source direction in the fitting procedure. Figures 2 and 3 show the fits to the double differential neutron multiplicity spectra at various angles for the two reactions. The post-scission multiplicity and the temperatures were assumed to be the same for both fission fragments and the total multiplicity was derived as $M_n^{\mathrm{tot}} = M_n^{\mathrm{pre}} + 2M_n^{\mathrm{post}}$. The observed neutron multiplicities are presented in Table I. The pre-scission neutron multiplicity is found to be higher for the system with entrance channel mass asymmetry $\alpha \leqslant \alpha_{\mathrm{BG}}$ as compared to the system lying on the other side (i.e., $\alpha \geqslant \alpha_{\mathrm{BG}}$). This difference in multiplicities increases with the excitation energy of the CN.

TABLE I. Values of neutron multiplicities for the two reactions.

	^{16}O + ^{181}Ta ($\alpha \geqslant \alpha_{\mathrm{BG}}$)			^{19}F + ^{178}Hf ($\alpha \leqslant \alpha_{\mathrm{BG}}$)		
E^*	M_n^{pre}	$2 \times M_n^{\mathrm{post}}$	M_n^{tot}	M_n^{pre}	$2 \times M_n^{\mathrm{post}}$	M_n^{tot}
72.0	2.58 ± 0.13	2.95 ± 0.15	5.58 ± 0.20	2.75 ± 0.16	2.84 ± 0.12	5.59 ± 0.20
76.0	2.79 ± 0.10	3.00 ± 0.12	5.79 ± 0.15	3.07 ± 0.13	3.05 ± 0.14	6.12 ± 0.19
81.0	3.10 ± 0.13	3.18 ± 0.11	6.28 ± 0.17	3.57 ± 0.12	3.15 ± 0.11	6.72 ± 0.16

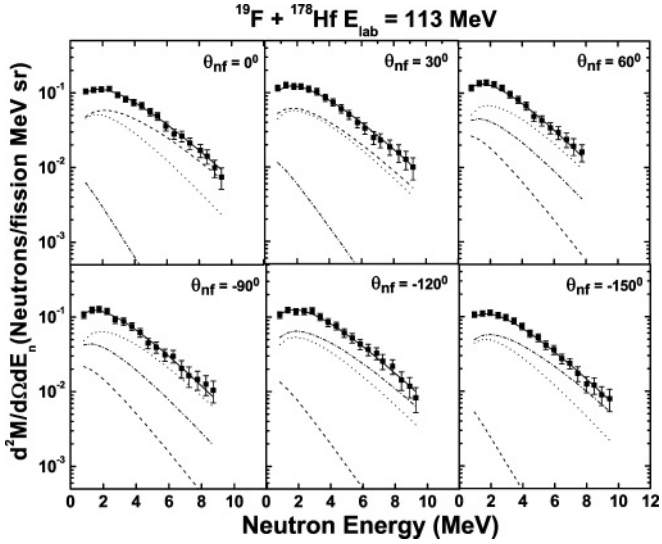

FIG. 3. Neutron multiplicity spectra (filled squares) for ^{19}F + ^{178}Hf at $E_{\rm lab} = 113$ MeV along with fits for pre-scission (dotted curve) and post-scission: fragment 1 (dashed curve) and fragment 2 (dot dashed curve). Solid curve represents the total contribution.

IV. STATISTICAL MODEL ANALYSIS

We have compared the experimental neutron multiplicities with the statistical model predictions for the decay of a CN. In addition to fission, evaporation of neutrons and statistical giant dipole γ rays were the other decay channels of the excited CN in our calculation. The neutron and GDR γ partial decay widths were obtained from the standard Weisskopf formula as given in Ref. [32], and the partial fission width was obtained from the Kramers modified Bohr-Wheeler formula [22], which includes the effect of nuclear dissipation on fission and is given as

$$\Gamma_f^{\rm Kramers} = \Gamma_f^{\rm BW}[(1+\gamma^2)^{1/2} - \gamma]. \tag{2}$$

In this equation, γ determines the strength of dissipation and was treated as a free parameter in the calculation. The Bohr-Wheeler fission width was calculated using the fission barrier obtained from the finite range liquid drop model [33] for the nuclear potential. Using these partial widths, we followed the time evolution of the CN in a statistical model code [34,35] until either fission occurred or an evaporation residue was formed.

The spin distribution of the CN was assumed to follow the usual Fermi distribution, the parameters of which were fixed by fitting the experimental fusion cross section [36]. The level density parameter was taken from the works of Ignatyuk *et al.* [37,38], who proposed a form that reflects the nuclear shell structure effects at low excitation energies and is given as follows:

$$a(U) = \tilde{a}\left(1 + \frac{f(U)}{U}\delta W\right),$$
$$f(U) = 1 - \exp(-U/E_D), \tag{3}$$

where U is the thermal energy of the CN, δW is the shell correction taken from the difference between the experimental and liquid drop model masses, E_D accounts for the rate at which the shell effect melts away with increase of excitation energy, and $\tilde{a}$ is the asymptotic value to which the level density parameter approaches with increasing excitation energy of the CN. The asymptotic level density parameter $\tilde{a}$ depends on the nuclear mass, shape, and pairing energy in a fashion similar to that of the liquid drop mass [39].

In a dissipative dynamical model of nuclear fission, the Kramers modified fission width is reached after a buildup or transient time period given as [40,41]

$$\tau_f = \beta/2\omega_1^2 \ln(10B_f/T), \tag{4}$$

where ω_1 is the frequency defining the shape of the angular-momentum-dependent fission barrier B_f, and T is the nuclear temperature. The value of ω_1 was taken as $\omega_1 = 10^{21}$/s, which was found [20] to be appropriate in the mass region under consideration. The buildup time was then incorporated into a dynamical fission width parametrized as [19]

$$\Gamma_f(t) = [1 - \exp(-2.3t/\tau_f)]\Gamma_f^{\rm Kramers}, \tag{5}$$

which was used in the evolution of the CN in the statistical model code. In this definition of the fission width, fission is considered to have taken place when the CN crosses the saddle point deformation. During transition from saddle to scission, the CN can emit further neutrons, which would contribute to the pre-scission multiplicity. The saddle-to-scission time interval is given as [18]

$$\tau_{\rm ssc} = \tau_{\rm ssc}^{\circ}[(1+\gamma^2)^{1/2} + \gamma]. \tag{6}$$

Here, $\tau_{\rm ssc}^{\circ}$ is the nondissipative saddle-to-scission time and its value is given as [41]

$$\tau_{\rm ssc}^{\circ} = \frac{2}{\omega_0} R[(\Delta V/T)^{1/2}], \tag{7}$$

where

$$R(z) = \int_0^z \exp(y^2)dy \int_y^{\infty} \exp(-x^2)dx \tag{8}$$

and ΔV is the potential energy difference between the saddle and scission points. Using this saddle-to-scission time interval, we have calculated the number of neutrons emitted during this period. We have also calculated the multiplicity of neutrons emitted from the fission fragments (post-scission neutrons). Based on symmetric fission, the statistical emission of neutrons from an excited fragment was followed until the excitation energy in the fragment dropped below the neutron emission threshold.

The excitation function of pre-scission neutron multiplicity calculated for different values of the dissipation strength γ for the reactions ^{16}O + ^{181}Ta and ^{19}F + ^{178}Hf are compared with the experimental values in Fig. 4. The comparison of the calculated post-scission neutron multiplicities with the experimental values is given in Fig. 5. It may be noted that the post-scission multiplicity also depends on γ, since the available excitation energy of the fission fragments is determined by the number of pre-scission neutrons. We find that a value of 0.4 for γ gives a reasonable fit to the experimental post-scission neutron multiplicity for the

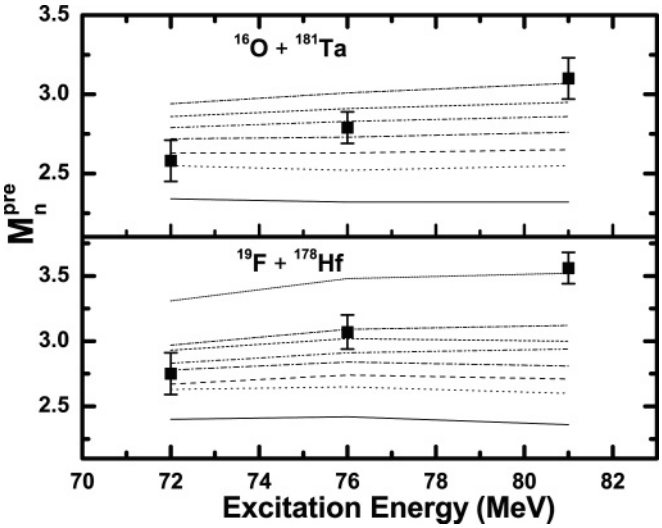

FIG. 4. Experimental pre-scission neutron multiplicities (filled squares) along with the statistical model calculation results for $\gamma = 0$ (solid line), $\gamma = 0.2$ (dotted line), $\gamma = 0.3$ (dashed line), $\gamma = 0.4$ (dash dotted line), $\gamma = 0.5$ (dash double dotted line), $\gamma = 0.6$ (short dashed line), $\gamma = 0.7$ (short dash dotted line), and $\gamma = 1.2$ (short dotted line).

^{16}O + ^{181}Ta system at all three energies whereas a value of 0.3 is required for the ^{19}F + ^{178}Hf system.

Comparing the calculated pre-scission neutron multiplicities with the experimental values, we first note that the predictions using the statistical model fission width ($\gamma = 0$) considerably underestimate the pre-scission neutron multiplicity at all three energies and the discrepancy increases with excitation energy. It is also observed that for each system, the experimental values at all three energies cannot be reproduced by a single value of γ. The best-fit values of γ for ^{16}O + ^{181}Ta at the three excitation energies are 0.2, 0.5, and 0.7, respectively, and those for ^{19}F + ^{178}Hf are 0.3, 0.7,

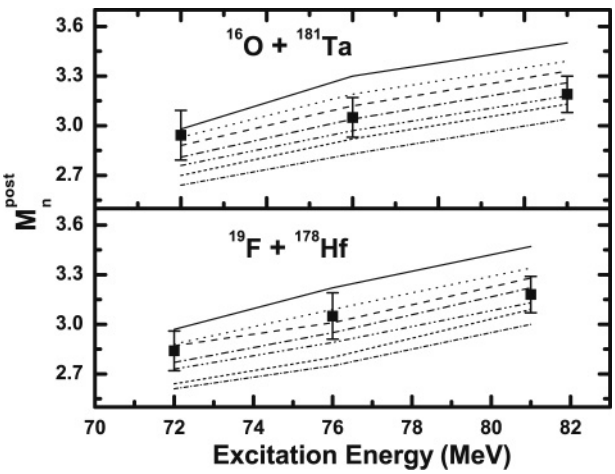

FIG. 5. Experimental post-scission neutron multiplicities (filled squares) along with the statistical model calculation results for $\gamma = 0$ (solid line), $\gamma = 0.2$ (dotted line), $\gamma = 0.3$ (dashed line), $\gamma = 0.4$ (dash dotted line), $\gamma = 0.5$ (dash double dotted line), $\gamma = 0.6$ (short dashed line), and $\gamma = 0.7$ (short dash dotted line).

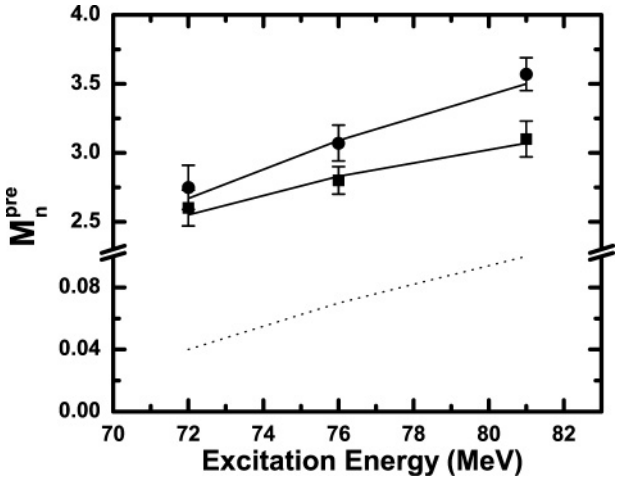

FIG. 6. The experimental pre-scission neutron multiplicities from the reactions ^{19}F + ^{178}Hf (solid circles) and ^{16}O + ^{181}Ta (solid squares) along with the fitted values from the statistical model calculation (solid line). The calculated multiplicities of neutrons emitted during saddle-to-scission transition for the two reactions are not distinguishable and are shown by the dotted line.

and 1.2, respectively. The experimental pre-scission neutron multiplicities along with the fitted values are shown in Fig. 6. To account for the systematic difference in the pre-scission multiplicity values for the two systems under consideration, we have next investigated the role of saddle-to-scission neutrons. Since the saddle-to-scission transition time depends on the CN spin and the spin distributions in the CN ^{197}Tl formed in the two reactions are different, the number of saddle-to-scission neutrons in the two reactions could be different. The calculated neutron multiplicities during saddle-to-scission transition are also shown in Fig. 6. We find that the saddle-to-scission contributions are almost the same for the two systems while they account for a small fraction of the total pre-scission neutrons. We therefore conclude that the observed difference in the pre-scission multiplicities cannot be attributed to the neutrons emitted during saddle-to-scission transition.

We have next plotted in Fig. 7 the γ values that reproduce the experimental pre-scission neutron multiplicities at the three excitation energies for the two systems. The statistical error associated with an experimental multiplicity gives rise to an error on the corresponding fitted value of γ and it is also shown in this figure. It is observed that starting with values that are very close for the two systems at the lowest excitation energy, γ increases faster with excitation energy for the ^{19}F + ^{178}Hf system than for the ^{16}O + ^{181}Ta system. To understand this systematic behavior of γ qualitatively, we first note that, though γ is introduced in the present calculation as the strength of the dissipative force in the fission dynamics of the CN, its value obtained from fitting the experimental data has to account for the total number of neutrons emitted before scission including those emitted during the formation time of the CN. Since the survival probability of a CN decreases quickly with increasing excitation energy, the formation time would be a larger fraction of the total time available for pre-scission neutron emission at a higher excitation energy. One would therefore expect the fraction of pre-scission neutrons emitted

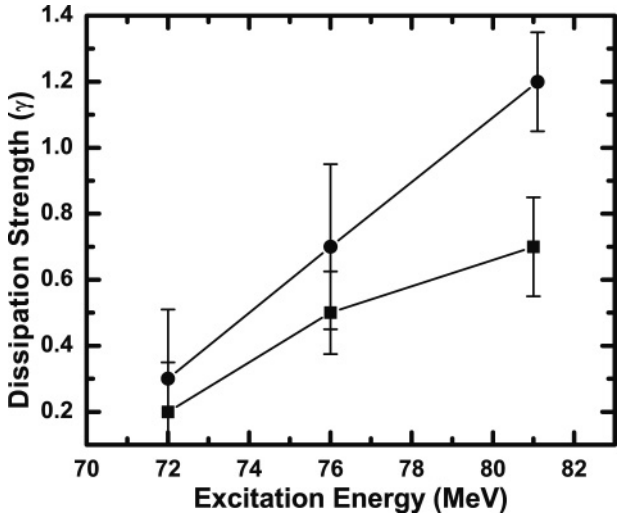

FIG. 7. The best-fit values of γ obtained for the systems $^{19}\mathrm{F} + {}^{178}\mathrm{Hf}$ (solid circles) and $^{16}\mathrm{O} + {}^{181}\mathrm{Ta}$ (solid squares). The lines are drawn to guide the eye.

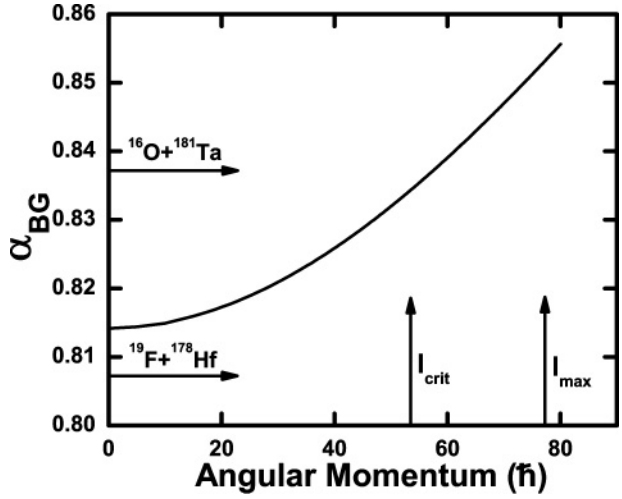

FIG. 8. L dependence of the Businaro-Gallone point.

during the formation time to increase with excitation energy. A larger value of γ is thus required to fit the experimental multiplicities at higher excitation energies to account for the larger number of pre-scission neutrons emitted during the formation time.

It may further be noted that the formation time, and hence the number of neutrons emitted during the formation time, would be different for two different systems leading to the same CN since the dynamics of their entrance channels are different. We would however expect the number of neutrons emitted after the fully equilibrated CN is formed to be the same for both systems considered in the present study since the same CN nucleus is formed at the same excitation energies. Consequently, the γ values extracted for the two systems at each excitation energy would be different on account of the difference in the formation time. This difference would grow with increasing excitation energy, reflecting the fact that the two systems have different formation time. In fact, we find in Fig. 7 that γ increases faster with excitation energy for the $^{19}\mathrm{F} + {}^{178}\mathrm{Hf}$ system than for the $^{16}\mathrm{O} + {}^{181}\mathrm{Ta}$ system. This indicates that the formation time for the more symmetric $^{19}\mathrm{F} + {}^{178}\mathrm{Hf}$ system is larger than that of $^{16}\mathrm{O} + {}^{181}\mathrm{Ta}$.

It may be mentioned at this point that microscopic theories of nuclear dissipation such as that of two-body viscosity can give rise to an excitation energy dependence of γ. It is therefore not the excitation energy dependence of γ but the difference in the excitation energy dependence between the two systems that is considered here as a signature of entrance channel effect on the multiplicity of pre-scission neutrons.

Since the entrance channel dynamics critically depends on the entrance channel mass asymmetry with respect to the Businaro-Gallone point, we shall now examine how this point moves with increasing angular momentum of the dinuclear system. Figure 8 shows the angular momentum dependence of the Businaro-Gallone point [26]. The largest value of the critical angular momentum encountered in the present study is also shown in this figure. The maximum angular momentum that leads to fusion is also indicated in Fig. 8. It is observed that both the $^{16}\mathrm{O} + {}^{181}\mathrm{Ta}$ and $^{19}\mathrm{F} + {}^{178}\mathrm{Hf}$ systems are on either side of the Businaro-Gallone line for the entire range of angular momentum accessible in the present study. Entrance channel effects are therefore expected to persist at all three beam energies considered in this work. However, it is also observed that both systems can be found on the same side of the Businaro-Gallone line at higher values of angular momentum in the range of $60\hbar$ to $75\hbar$. One can therefore speculate that a reduction in the entrance channel effects may be experimentally observed at higher beam energies.

We next performed statistical model calculations using a temperature-dependent level density parameter. Since our previous conclusion regarding the entrance channel effect relies on the excitation energy dependence of γ, it is important to verify whether the same conclusion holds when a temperature-dependent level density parameter is used in the calculation. The excitation energy dependence as given in Eq. (3) is relatively weak since it merely accounts for the smoothing away of the nuclear shell structure. However, the temperature dependence may be much stronger, as was indicated by Thomas-Fermi calculations [42]. Thus an additional temperature-dependent factor that retains the good agreement with low-energy level density data is included in our calculation. The final form of the level density parameter is then

$$\begin{aligned} a(T) &= a(U)[1 - \kappa f(T)], \\ f(T) &= 1 - \exp[-(TA^{1/3}/21)^2], \end{aligned} \tag{9}$$

where $a(U)$ is calculated according to Eq. (3) and κ determines the strength of the additional temperature dependence. This expression for the level density parameter is obtained from the energy dependence of the mean-field parameters in Ref. [42]. Values of κ in the range $0.4 - 0.8$ have been used in earlier works [19]. We have used $\kappa = 0.8$ in the present calculation.

Using the level density parameter as given in Eq. (10), we subsequently adjusted the strength of γ to reproduce

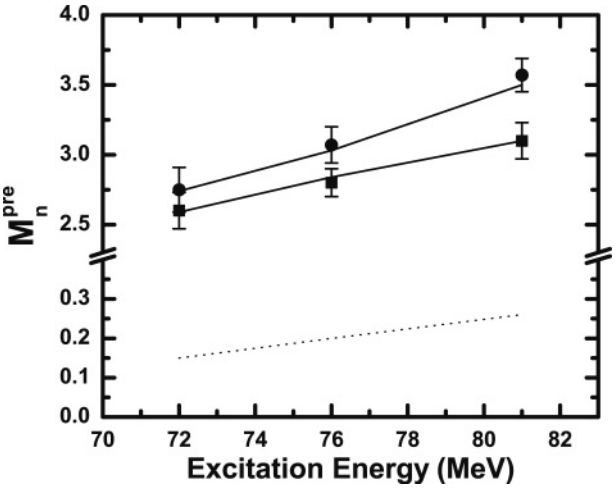

FIG. 9. The experimental pre-scission neutron multiplicities from the reactions $^{19}F + ^{178}Hf$ (solid circles) and $^{16}O + ^{181}Ta$ (solid squares) along with the fitted values from the statistical model calculation (solid line) using a value of $\kappa = 0.8$ for the temperature dependence of the level density parameter (see text). The calculated multiplicities of neutrons emitted during saddle-to-scission transition for the two reactions are not distinguishable and are shown by the dotted line.

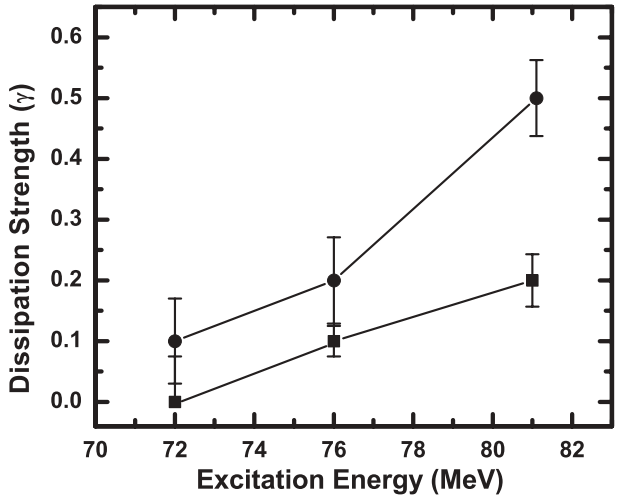

FIG. 10. The best-fit values of γ obtained from statistical model calculation using a value of $\kappa = 0.8$ (see text) for the systems $^{19}F + ^{178}Hf$ (solid circles) and $^{16}O + ^{181}Ta$ (solid squares). The lines are drawn to guide the eye.

the experimental pre-scission neutron multiplicity at each excitation energy; the results are shown in Fig. 9. The calculated values of the multiplicity of neutrons emitted during saddle-to-scission transition of the CN are also shown in this figure. We find that the number of neutrons emitted during the saddle-to-scission transition does not depend on the entrance channel and is a small fraction of the total number of pre-scission neutrons, similar to our observation in Fig. 6 earlier. It is however interesting to note that more neutrons are emitted during saddle-to-scission transition when calculations are performed with $\kappa = 0.8$ compared to those obtained with $\kappa = 0$ (Fig. 6). This is because the level density parameter with $\kappa = 0.8$ is smaller than that obtained with $\kappa = 0$ and hence the temperature calculated with the former is higher than that with the later. More neutrons are emitted from a CN at a higher temperature than from one at a lower temperature over a given interval of time (saddle-to-scission transition time).

Lastly, the values of γ obtained with $\kappa = 0.8$ and that reproduce the experimental pre-scission neutron multiplicities are shown in Fig. 10 for both systems. Evidently, γ is lower for $\kappa = 0.8$ than for $\kappa = 0$ (see Fig. 7). This is not unexpected since it is well known that results from statistical model calculations are sensitive to the level density parameter. It is, however, interesting to note that γ increases faster with excitation energy for the $^{19}F + ^{178}Hf$ system than for the $^{16}O + ^{181}Ta$ system, similar to our earlier observation in Fig. 7, which corresponds to a larger formation time for the $^{19}F + ^{178}Hf$ system than for $^{16}O + ^{181}Ta$. Thus the distinguishing features of entrance channel effects are retained in the statistical model calculations with different temperature dependencies on the level density parameter.

V. SUMMARY AND CONCLUSIONS

We have measured the multiplicities of pre- and post-scission neutrons emitted in the fission of the ^{197}Tl compound nucleus. This CN was formed at the same excitation energies in $^{16}O + ^{181}Ta$ and $^{19}F + ^{178}Hf$ reactions using ^{16}O beam at energies of 105, 110, and 115 MeV and ^{19}F beam at 108, 113, and 118 MeV, respectively. The pre-scission neutron yield from the two systems lying on either side of the Businaro-Gallone point was found to be different, reflecting its dependence on the mass asymmetry in the entrance channel. The experimental neutron multiplicities were compared with the statistical model predictions that included a dissipative force in the fission channel. The strength of the dissipation, γ, was obtained by fitting the experimental data. The strength γ was found to increase with excitation energy for both systems though the rate of increase was higher for $^{19}F + ^{178}Hf$ than for $^{16}O + ^{181}Ta$. It was then shown from the statistical model calculation that the number of neutrons emitted during the saddle-to-scission transition were the same for the two systems and hence they could not account for the observed pre-scission multiplicity difference between the two systems. We therefore concluded that the observed difference can be solely attributed to the different entrance channel dynamics of the two systems. Subsequently, we argued that the excitation energy dependence of γ should depend on the formation time of the CN. Therefore, the observed difference in the excitation energy dependence of γ between the two systems can be considered as evidence of a larger formation time for a CN formed in a less asymmetric entrance channel ($\alpha < \alpha_{BG}$) compared to one formed in an entrance channel with higher asymmetry ($\alpha > \alpha_{BG}$).

ACKNOWLEDGMENTS

We are thankful to the accelerator group of IUAC for providing good-quality pulsed beams. The help received from

Mr. Abhilash in target preparation and Mr. P. Barua in setting up the experimental configuration in GPSC is gratefully acknowledged. We are thankful to Dr. V. S. Ramamurthy for useful discussion on this work. We would like to thank the Department of Science and Technology (DST), New Delhi, and the Council of Scientific and Industrial Research (CSIR), New Delhi, for financial support to carry out this work.

[1] H. Rossner, D. Hilscher, D. J. Hinde, B. Gebauer, M. Lehmann, M. Wilpert, and E. Mordhorst, Phys. Rev. C **40**, 2629 (1989).
[2] D. J. Hinde, D. Hilscher, H. Rossner, B. Gebauer, M. Lehmann, and M. Wilpert, Phys. Rev. C **45**, 1229 (1992).
[3] A. Saxena, A. Chatterjee, R. K. Choudhury, S. S. Kapoor, and D. M. Nadkarni, Phys. Rev. C **49**, 932 (1994).
[4] D. Hilscher, H. Rossner, B. Cramer, U. Jahnke, M. Lehmann, E. Schwinn, M. Wilpert, T. Wilpert, H. Frobeen, E. Mordhorst *et al*., Phys. Rev. Lett. **62**, 1099 (1989).
[5] D. J. Hinde, H. Ogata, M. Tanaka, T. Shimoda, N. Takahashi, A. Shinohara, S. Wakamatsu, K. Katori, and H. Okamwra, Phys. Rev. C **39**, 2268 (1989).
[6] L. M. Pant, A. Saxena, R. G. Thomas, D. C. Biswas, and R. K. Choudhury, Eur. Phys. J. A **16**, 43 (2003).
[7] J. O. Newton, Pramana **33**, 175 (1989).
[8] J. Cabrera, T. Keutgen, Y. E. Masri, C. Dufauquez, V. Roberfroid, I. Tilquin, J. V. Mol, R. Regimbart, R. J. Charity, J. B. Natowitz *et al*., Phys. Rev. C **68**, 034613 (2003).
[9] D. Hilscher and H. Rossner, Ann. Phys. (Paris) **17**, 471 (1992).
[10] J. P. Lestone, Phys. Rev. Lett. **70**, 2245 (1993).
[11] J. P. Lestone, J. R. Leigh, J. O. Newton, D. J. Hinde, J. X. Wei, J. X. Chen, S. Elfstorm, and M. Zielinska-Pfabe, Nucl. Phys. **A559**, 277 (1993).
[12] A. Saxena, D. Fabris, G. Prete, D. V. Shetty, G. Viesti, B. K. Nayak, D. C. Biswas, R. K. Choudhury, S. S. Kapoor, and M. L. *et al*., Nucl. Phys. **A730**, 299 (2004).
[13] A. Chatterjee, A. Navin, S. Kailas, P. Singh, D. C. Biswas, A. Karnik, and S. S. Kapoor, Phys. Rev. C **52**, 3167 (1995).
[14] K. Ramachandran, A. Chatterjee, A. Navin, K. Mahata, A. Shrivastava, V. Tripathy, S. Kailas, V. Nanal, R. G. Pillay, A. Saxena *et al*., Phys. Rev. C **73**, 064609 (2006).
[15] M. Thoennessen, D. R. Chakrabarty, M. G. Herman, R. Butsch, and P. Paul, Phys. Rev. Lett. **59**, 2860 (1987).
[16] R. Butsch, M. Thoennessen, D. R. Chakrabarty, M. G. Herman, and P. Paul, Phys. Rev. C **41**, 1530 (1990).
[17] R. Butsch, D. J. Hofman, C. P. Montoya, P. Paul, and M. Thoennessen, Phys. Rev. C **44**, 1515 (1991).
[18] D. J. Hofman, B. B. Back, and P. Paul, Phys. Rev. C **51**, 2597 (1995).
[19] I. Diószegi, N. P. Shaw, I. Mazumdar, A. Hatzikoutelis, and P. Paul, Phys. Rev. C **61**, 024613 (2000).
[20] I. Diószegi, N. P. Shaw, A. Bracco, F. Camera, S. Tettoni, M. Mattiuzzi, and P. Paul, Phys. Rev. C **63**, 014611 (2000).
[21] N. Bohr and J. A. Wheeler, Phys. Rev. **56**, 426 (1939).
[22] H. A. Kramers, Physica (Utrecht) **7**, 284 (1940).
[23] T. Wada, Y. Abe, and N. Carjan, Phys. Rev. Lett. **70**, 3538 (1993).
[24] V. S. Ramamurthy, S. S. Kapoor, R. K. Choudhury, A. Saxena, D. M. Nadkarni, A. K. Mohanty, B. K. Nayak, S. V. S. Sastry, S. Kailas, A. Chatterjee *et al*., Phys. Rev. Lett. **65**, 25 (1990).
[25] K. T. R. Davies and A. J. Sierk, Phys. Rev. C **31**, 915 (1985).
[26] M. Abe, KEK Report No. 86-26, KEK TH-28, 1986.
[27] A. Jhingan, P. Sugathan, K. S. Golda, S. A. Khan, T. Varughese, and E. T. Subramaniam, DAE Symp. Nucl. Phys. **47B**, 564 (2004).
[28] T. G. Masterson, Nucl. Instrum. Methods **88**, 61 (1970).
[29] R. A. Cecil, B. D. Anderson, and R. Madey, Nucl. Instrum. Methods **161**, 439 (1979).
[30] K. S. Golda, H. Singh, R. P. Singh, S. K. Datta, and R. K. Bhowmik, DAE Symp. Nucl. Phys. **50**, 445 (2005).
[31] V. E. Viola, K. Kwiatkowski, and M. Walker, Phys. Rev. C **31**, 1550 (1985).
[32] P. Frobrich and I. I. Gontchar, Phys. Rep. **292**, 131 (1998).
[33] A. J. Sierk, Phys. Rev. C **33**, 2039 (1986).
[34] G. Chaudhuri and S. Pal, Phys. Rev. C **63**, 064603 (2001).
[35] G. Chaudhuri and S. Pal, Phys. Rev. C **65**, 054612 (2002).
[36] B. R. Behera, S. Jena, M. Satpathy, S. Roy, P. Basu, M. K. Sharan, M. L. Chatterjee, S. Kailas, K. Mahata, and S. K. Datta, Phys. Rev. C **66**, 047602 (2002).
[37] A. V. Ignatyuk, M. G. Itkis, V. N. Okolovich, G. N. Smirenkin, and A. Tishin, Yad. Fiz. **21**, 485 (1975).
[38] A. V. Ignatyuk, M. G. Itkis, V. N. Okolovich, G. N. Smirenkin, and A. Tishin, Sov. J. Nucl. Phys. **21**, 255 (1975).
[39] W. Reisdorf, Z. Phys. A **300**, 227 (1981).
[40] K. H. Bhatt, P. Grangé, and B. Hiller, Phys. Rev. C **33**, 954 (1986).
[41] P. Grangé, S. Hassani, H. A. Weidenmuller, A. Gavron, J. R. Nix, and A. J. Sierk, Phys. Rev. C **34**, 209 (1986).
[42] S. Shlomo and J. B. Natowitz, Phys. Rev. C **44**, 2878 (1991).